ICMIEE20-258

Computational Analysis of Horizontal Axis Wind Turbine Blade Profiles at Low Wind Speed

Aoyon Paul[*]*, Turjo Ghoshal, Md. Mahadi Hassan*
Department of Mechanical Engineering, Chittagong University of Engineering & Technology, Chittagong-4349, BANGLADESH

ABSTRACT
To ensure the maximum energy efficiency and find the optimum operating conditions of a wind turbine, an analysis of the blade profile of a horizontal axis wind turbine was carried out. In this study, a wind turbine blade's root and tip profiles were simulated to find the aerodynamic characteristics such as coefficient of lift (C_L), coefficient of drag (C_D), and sliding ratio (C_L/C_D) at different angle of attacks and wind speeds. A computational analysis of NREL's S822 and S823 airfoils were performed to find the range of suitable operating angle of attack at low wind speed. The analysis showed that when the two-airfoil profiles were used in the same wind turbine blade, the operating angle of attack is preferable to lie between 6° to 8° for a wind velocity of 3, 4 and 5 m/s, respectively. S823 airfoil showed good aerodynamic characteristics compared to S822 airfoil. NREL's S823 (Root) and S822 (Tip) airfoils can be used in a wind turbine having a blade length of 1 to 5 m to extract energy from wind.

Keywords: Airfoil, Angle of Attack, CFD, HAWT, Sliding ratio

1. Introduction

The energy crisis is one of the predominant issues of the 21st century all over the world. Most of the country of the world including Bangladesh depends largely on fossil fuel-based energy sources [1]. From the recent studies, it can be seen that, in Bangladesh 65% of the power generated from only Gas and Coal which are fossil fuels [2]. But there is no unlimited source of fossil fuel, it will be finished after a certain time [3]. As a result, most countries try to focus on renewable energy sources. Among all, wind energy is one of the sustainable renewable energy sources [4]. Being a tropical country Bangladesh has a different kind of wind flow in different seasons all over the year. During Monsoon, the strong south/south-westerly wind coming from the Indian Ocean; enters into Asia. This wind passes through the coastal area of Bangladesh. This wind blows over the surface of Bangladesh from March to September, having an average speed of 3 m/s to 6 m/s [5]. From October to February, wind speed remains relatively lower. The maximum wind speed is gained during June-July [5]. It was found that the generated wind map and the modified ground data resemble. Annual average wind speed at 30 m height along the coastal belt is above 5 m/s. Wind speed in northeastern parts is above 4.5 m/s while inland wind speed is around 3.5 m/s for most part of Bangladesh [6]. In the world market, the usage of wind energy is increasing vastly as a low-density power source. In this respect, the efficiency of this energy source must be ensured. Wind turbine, a possible green technology can help reduce our dependence on fossil fuels and counter the serious danger to humans and biodiversity faced by climate change.

The rotor blade is one of the most important parts of the wind turbine which is the primary energy conversion device. For the wind turbine blade design, the selection of airfoils for different sections and the distribution of chords and twists are pivotal [7]. For this the aerodynamics characteristics and perspectives of a wind turbine along with the flow around and downstream needed to be analyzed. Most of the researcher focused on wind turbines which have long blade length. But there is limited research on small wind turbines. The NREL's S822 and S823 airfoils are recommended to use in a wind turbine blade which length range is 1 to 5 m. This type of wind turbine has a generator of size 2-20kW [8]. In this study, the CFD analysis was taken over of the NREL's S822 airfoil as tip and S823 airfoil as root respectively of a horizontal axis wind turbine blade of length 1 to 5 m. The aerodynamics characteristics such as the coefficient of drag, coefficient of lift, sliding ratio, and angle of attack are analyzed under low wind speed conditions (3, 4 and 5 ms^{-1}). The motive of this study was to observe the behavior of the wind turbine's blade profile at low wind speeds which will be suitable for Asian countries like Bangladesh. The CFD analysis was carried out in ANSYS 2020 R2 student version software.

2. Background

When air flows over an airfoil surface, due to velocity alternation positive and negative pressure generates along the airfoil surface from the leading edge to trailing edge. The net force is found by integrating the pressure over the airfoil surface. The vertical component of this net force is called lift force and the horizontal component is called drag force.

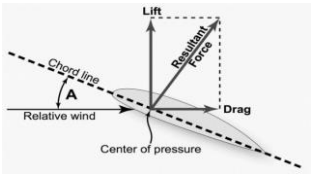

* Corresponding author. Tel.: +88-01680534809
E-mail address: aoyonpaul@gmail.com

Fig.1 Resultant aerodynamic force and its components [9]

Lift and drag coefficient are defined as,

Lift coefficient,

$$C_L = \frac{F_L}{\frac{1}{2}\rho V^2 c} \quad (1)$$

Drag coefficient,

$$C_D = \frac{F_D}{\frac{1}{2}\rho V^2 c} \quad (2)$$

The ratio of C_L and C_D is called sliding ratio, which is represented as,

$$\varepsilon = \frac{C_L}{C_D} \quad (3)$$

The flow physics in the wind turbine is different from the wing of an airplane. For specific wind speed, rotational velocity, ωR is less at the root (Fig.2a) than the tip (Fig. 2b) of a wind turbine blade.

Flow angle $\varphi = \alpha + \beta$, where α is the angle of attack and β is the blade's twisting angle with rotor plane. The flow angle will be changed when wind velocity will change (Fig. 2c). For a specific wind velocity, to prevent stall in the wind turbine needs proper angle of attack and twisting angle. When the flow angle increases, β or rotational speed of the blade needs to be changed so that the value of α will always less than the stall angle (Fig. 2d). Fig. 2 was created by Microsoft PowerPoint.

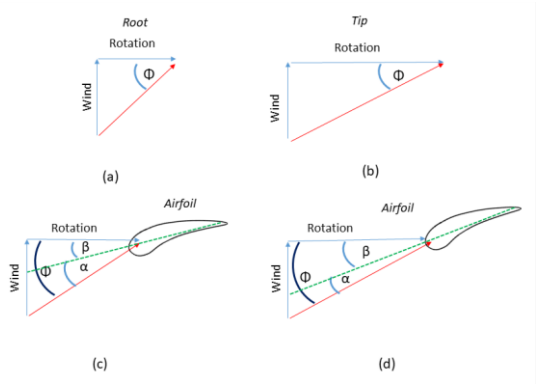

Fig.2 Velocity vector of an airfoil with wind velocity and blade rotation for a wind turbine.

3. Computational Approach

3.1 Profile selection and CAD model

The airfoils of the NACA 44XX, NACA 23XX, NACA 63XX, and NASA LS (1) series experience a significant loss of performance due to roughness effects resulting from leading-edge contamination [8].For minimizing energy loss NREL has developed some airfoil profile. S822 and S823 are recommended by NREL for a small size wind turbine with blade length 1-5 meters [8]. The airfoils coordinates were taken from the NREL database to create the 2D geometry [10, 11]. Then the coordinates were imported in the ANSYS design modeler. The length of the chord was set to 1m for both airfoils. Fig. 3 and Fig. 4 are exhibited the 2D representation of the S822 and S823 airfoils, consecutively.

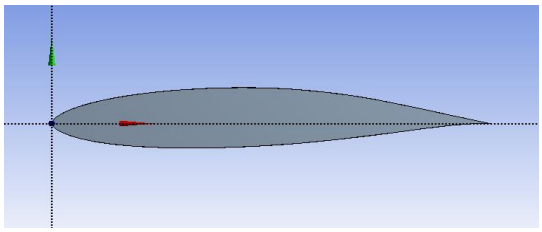

Fig.3 2D model of S822 airfoil

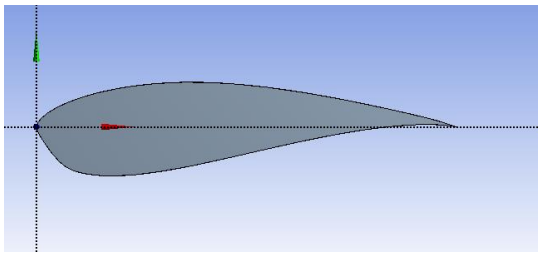

Fig.4 2D model of S823 airfoil

3.2 Mesh generation

Meshing is one of the most important steps in Computational Fluid Dynamics (CFD) analysis. The accuracy of the result varies when the mesh elements and nodes are changed. If the number of mesh elements and nodes is increased, then accuracy as well as computation time will also increase. In this analysis, structured C-mesh has been used. y^+ <1 was chosen for this analysis. Mesh density was higher near the airfoil surface to capture the near-surface flow physics. A total of 150000 mesh elements was used for both the S822 and S823 airfoils. Fig. 5 and Fig. 6 exhibit the mesh generated for S822 and S823 airfoils, consecutively.

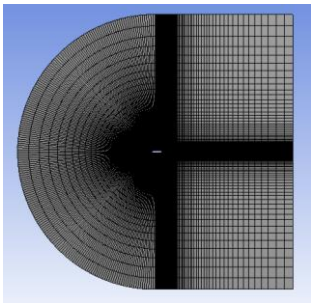

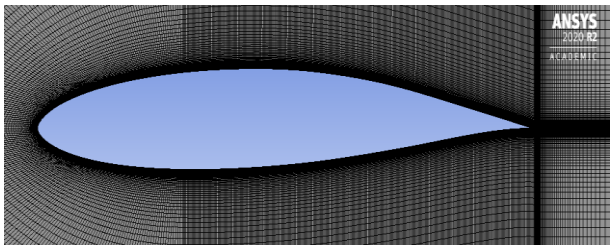

Fig.5 Meshing of S822 airfoil

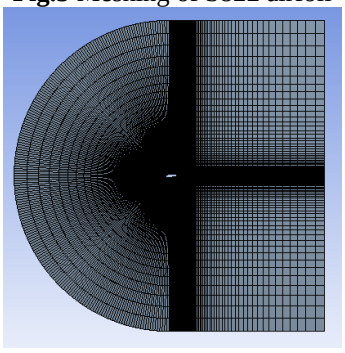

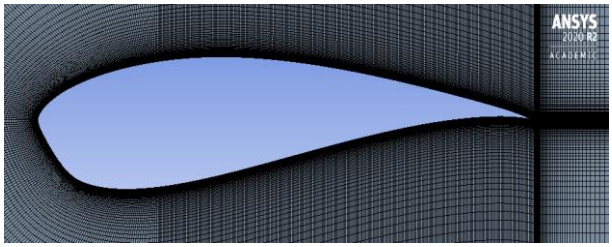

Fig.6 Meshing of S823 airfoil

3.3 Governing Equations

Conservation of momentum, mass, and energy equation contains the fundamental physics of flow in fluid dynamics. The energy equation can be neglected when the flow is assumed as isothermal. If Ma< 0.3, the flow can be assumed as incompressible.

Since density is constant, the continuity (Conservation of mass) equation can be written as,

$$\nabla . \underline{u} = 0 \quad (4)$$

$$\frac{\partial u}{\partial x} + \frac{\partial v}{\partial y} + \frac{\partial w}{\partial z} = 0 \quad (5)$$

The Navier-Stokes equation represents a partial differential form of the conservation of momentum. This equation can be written as,

$$\rho \frac{D\underline{u}}{Dt} = -\nabla . P + \mu \nabla^2 \underline{u} + \rho \underline{g} \quad (6)$$

Where, $\underline{u} = (u, v, w)$, $\underline{g} = (g_x, g_y, g_z)$

In the right-hand side of equation (6), the first two terms represent the internal force and the last term represent external or body force. And, the left-hand side represents the acceleration. This equation arises from applying Newton's second law to fluid motion.

During numerical analysis, Reynolds Averaged Navier-Stokes equations were used. SST K-omega turbulence model was used for solving RANS equations. The SST k-omega turbulence model has more accuracy than other models, where an adverse pressure gradient is present. This model provides a more accurate prediction of flow separation [12].

3.4 Boundary Conditions

Pressure based solver in ANSYS-Fluent was selected for this analysis because the flow was incompressible. Body force was neglected. The analysis was conducted for the inlet velocity 3, 4 and 5 m/s. Air density was 1.225 kg/m^3 and viscosity was 1.7894 x 10^{-5} N-s/m^2. In the airfoil surface, no slip boundary condition was applied. Gauge pressure was maintained 0 Pa at the outlet boundary.

In this analysis, Coupled-scheme was used. In the spatial discretization, least squared cell-based gradient was used. The pressure was second order along with momentum, turbulent kinetic energy, and specific turbulent dissipation rate was used as second order upwind. Hybrid initialization was selected for this study.

4. Results and Discussion

Computational analysis is performed on a wind turbine blade profile. In this analysis NREL's S822 airfoil used as a tip and S823 airfoil used as a root. For an unstructured mesh of 133378 elements, result varies approximately 12% compared with a structured mesh of 150000 elements.

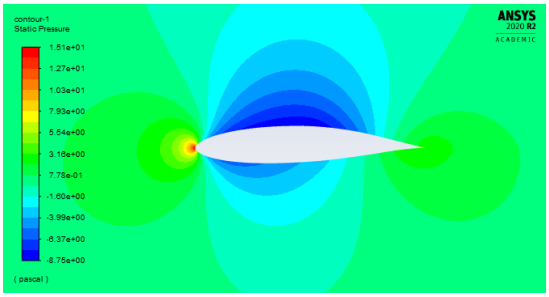

Fig.7 Pressure contour of S822 for 0° AOA at 5 m/s airflow velocity.

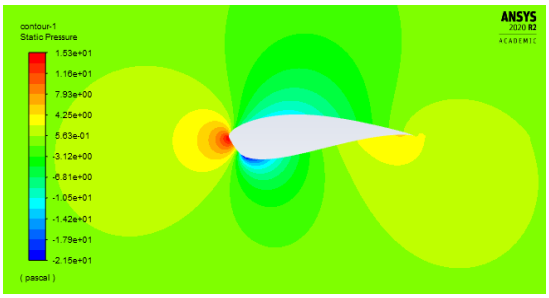

Fig.8 Pressure contour of S823 for 0° AOA at 5 m/s airflow velocity.

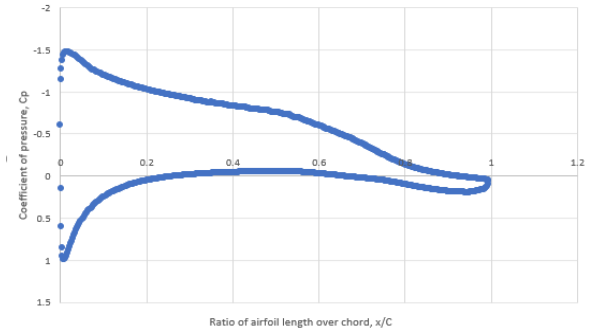

Fig.9 Pressure coefficient of S822 for 6° AOA at 5 m/s airflow velocity.

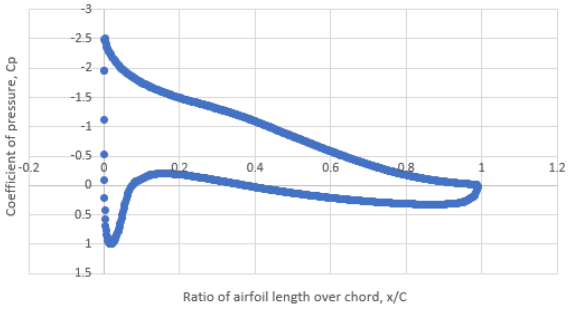

Fig.10 Pressure coefficient of S823 for 8° AOA at 5 m/s airflow velocity.

It is evident from Fig. 7 and Fig. 8 that the maximal pressure is observed at the leading edge for both S822 and S823 airfoils. Also, observed that there is negative pressure on both the top and bottom surfaces of the airfoils. In S822 there is more negative pressure on the top surface than the S823 airfoil at 0° AOA for 5 m/s velocity of air. From the Fig. 9 and Fig. 10, it is observed that the coefficient of pressure changed from leading to trailing edge for both airfoils. The imbalance of pressure on the upper and lower surfaces of the airfoils is the reason for generating the lift. This lift is increasing with the increasing of the AOA up to a specific point.

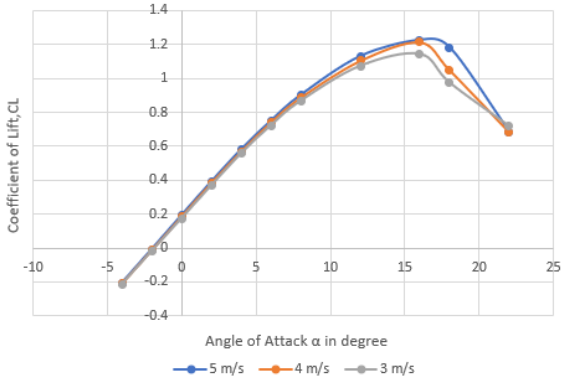

Fig.11 Computational lift coefficient for different AOA at 3, 4 and 5 m/s airflow velocity for S822 airfoil

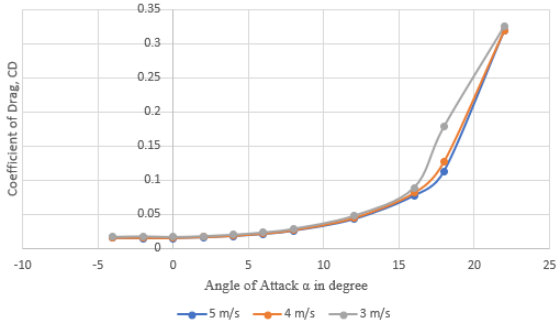

Fig.12 Computational drag coefficient for different AOA at 3, 4 and 5 m/s airflow velocity for S822 airfoil.

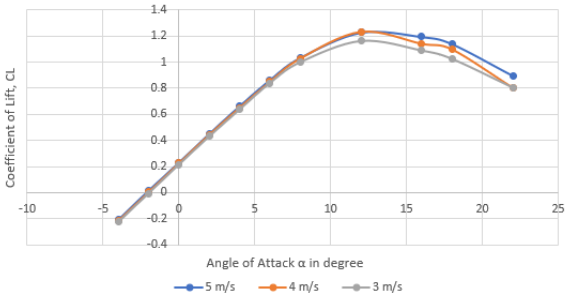

Fig.13 Computational lift coefficient for different AOA at 3, 4 and 5 m/s airflow velocity for S823 airfoil.

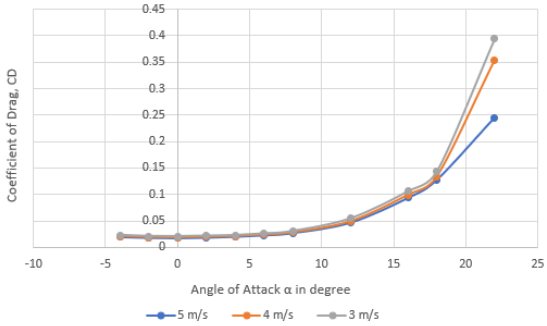

Fig.14 Computational drag coefficient for different AOA at 3, 4 and 5 m/s airflow velocity for S823 airfoil

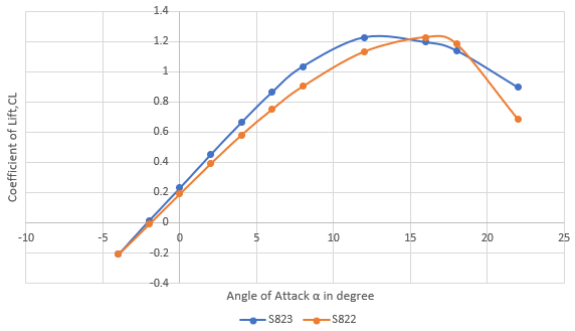

Fig.15 Lift coefficient of S823 and S822 airfoils for different AOA at 5 m/s airflow velocity

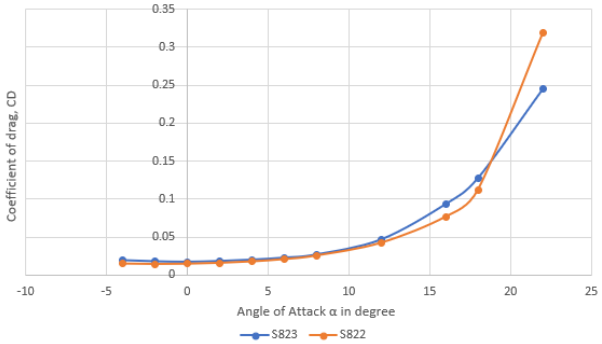

Fig.16 Drag coefficient of S823 and S822 airfoils for different AOA at 5 m/s airflow velocity

From the Fig. 11 and Fig. 13, it is noticed that the coefficient of lift increases with the increasing of angle of attack. The lift force helps the wind turbine blade to rotate. If the lift force is increased then the rotational speed of the wind turbine blade is also increased. Fig. 12 and Fig. 14 shows that, the coefficient of drag increases gradually with the increasing of angle of attack. Comparison of lift and drag coefficient of S822 and S823 airfoils are presented in Fig. 15 and Fig. 16.

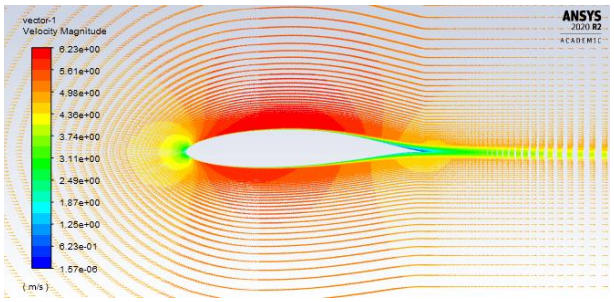

Fig.17 Velocity vectors of S822 airfoil for 0^{o} AOA at 5 m/s airflow velocity.

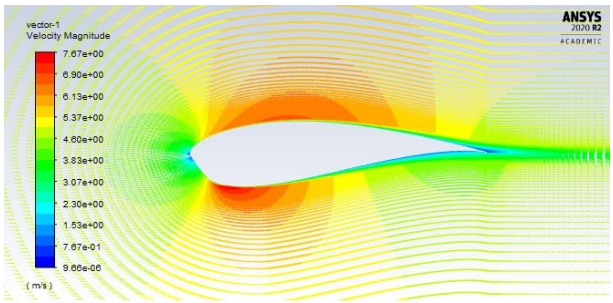

Fig.18 Velocity vectors of S823 airfoil for 0^{o} AOA at 5 m/s airflow velocity.

From the Fig. 17 and Fig. 18 it is observed that streamlines are detached from the upper and lower contact surface as the air flows over the trailing edge for both the airfoils. In this region, a slight negative pressure is created. This negative pressure produces subsequent wake at the separation point of the streamline of the airfoil. And this phenomenon increases the drag. As the angle of attack increases, the separated region is also increased rapidly which creates an obstacle to increase the lift. At this critical AOA, the separated flow region is so superior that the lift decreases and the drag increases rapidly. For this phenomenon, after increasing at a certain angle of attack the lift starts to decrease.

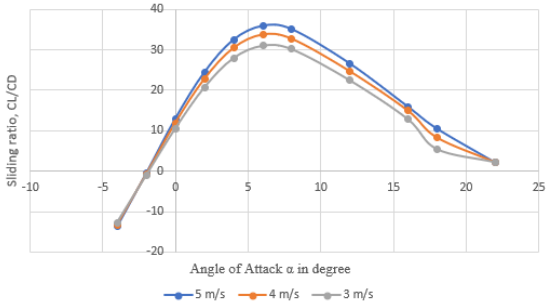

Fig.19 Sliding ratio of S822 airfoil for different AOA at 3, 4 and 5 m/s airflow velocity

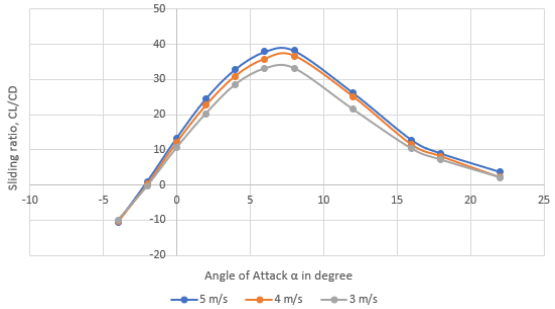

Fig.20 Sliding ratio of S823 airfoil for different AOA at 3, 4 and 5 m/s airflow velocity

The sliding ratio plays a vital role in the selection process of the airfoil profile. From Fig. 19 and Fig. 20, it is observed that, with the increase of AOA the sliding

ratio is also increased up to a certain point. For S822 airfoil maximum sliding ratio was noticed at 6° AOA. Also, for the S823 airfoil, the maximum sliding ratio was noticed at 8° AOA. After a certain angle of attack, the sliding ratio starts to decrease. In case of selecting a better airfoil profile, the sliding ratio must be higher compare to the other airfoil profiles.

The data found from this computational analysis approximately matches with NREL's experimental data. For S822 airfoil C_L varies up to 16% and C_D varies up to 10%, and for S823 airfoil C_L varies up to 2% and C_D varies up to 1% with compared to NREL's data [8, 13].

It can be observed that the two NREL's airfoils show almost similar characteristics at specific wind speeds. When the two airfoil profiles used in the same wind turbine blade, the operating angle of attack must lie between 6° to 8° and the Reynolds number between 2.1×10^5 to 3.42×10^5. So, S822 airfoil can be used as a tip and S823 airfoil can be used as a root for a wind turbine blade at low wind speeds. But in case of using a single airfoil profile for the whole wind turbine blade, S823 is slightly better than S822 because of a better sliding ratio for a specific wind speed.

5. Conclusions

From the overall analysis, it can be summarized that the sliding ratio is the most important parameter to determine the effectiveness of a wind turbine blade profile. Alongside, the angle of attack and wind speed also play an important role in the selection process of the wind turbine blade profile. When NREL's S822 and S823 airfoils are used combinedly in a wind turbine blade, the effective operating angle of attack should be 6^o to 8^o. Maximum energy can be extracted when the wind turbine operates at an effective operating angle of attack. For countries with low wind speeds like Bangladesh, horizontal axis wind turbines made of 1 to 5 m long blades will be effective if it can be operated between 6° to 8° angle of attack.

6. References

[1] T. Islam, S. A. Shahir, T. M. I. Uddin, and A. Z. A. Saifullah, "Current energy scenario and future prospect of renewable energy in Bangladesh," *Renew. Sustain. Energy Rev.*, vol. 39, pp. 1074–1088, 2014.

[2] A. Z. A. Saifullah, A. Karim, and R. Karim, "Wind Energy Potential in Bangladesh American Journal of Engineering Research (AJER)," no. 7, pp. 85–94, 2016.

[3] S. H. Mohr, J. Wang, G. Ellem, J. Ward, and D. Giurco, "Projection of world fossil fuels by country," *FUEL*, vol. 141, pp. 120–135, 2015.

[4] "S821 Airfoil Shape." Available: https://wind.nrel.gov/airfoils/Shapes/S821_Shape.html. (Accessed: 25-Aug-2020).

[5] S. E. E. Profile, "Prospects of Wind Energy in Bangladesh Prospects of Wind Energy in Bangladesh," no. June, 2018.

[6] M. J. Khan, M. T. Iqbal, and S. Mahboob, "A wind map of Bangladesh," *Renew. Energy*, vol. 29, no. 5, pp. 643–660, Apr. 2004.

[7] M. R. Ahmed, S. Narayan, A. Zullah, K. Maritime, Y. Lee, and K. Maritime, "Experimental and Numerical Studies on a Low Reynolds Number Airfoil for Wind Turbine," no. May 2014, 2011.

[8] J. L. Tangier and D. M. Somers, "NREL Airfoils Families for HAWTs," no. January, 1995.

[9] "How is an induced drag formed in an aerofoil? - Quora." Available: https://www.quora.com/How-is-an-induced-drag-formed-in-an-aerofoil. (Accessed: 23-Aug-2020).

[10] "S822 Airfoil Shape." Available: https://wind.nrel.gov/airfoils/Shapes/S822_Shape.html. (Accessed: 22-Aug-2020).

[11] "S823 Airfoil Shape." Available: https://wind.nrel.gov/airfoils/Shapes/S823_Shape.html. (Accessed: 25-Aug-2020).

[12] F. R. Menter, "Two-equation eddy-viscosity turbulence models for engineering applications," *AIAA J.*, vol. 32, no. 8, pp. 1598–1605, 1994.

[13] D. M. S. Airfoils, "The S822 and S823 Airfoils October 1992 — December 1993 The S822 and S823 Airfoils," no. December 1993, 2005.

NOMENCLATURE

AOA	: Angle of Attack
F_L	: Lift force, N
F_D	: Drag force, N
C_L	: Coefficient of lift
C_D	: Coefficient of drag
C_P	: Coefficient of pressure
Ma	: Mach number
V	: Air velocity, m/s
ρ	: Air density, kg/m^3
μ	: Viscosity, N.s/m^2
ω	: Rotational velocity, rad/s
R	: Rotor radius, m
c	: Chord length, m
HAWT	: Horizontal Axis Wind Turbine
NREL	: National Renewable Energy Laboratory
SST	: Shear Stress Transport